


Research Paper

Protection against Lethal Enterovirus 71 Challenge in Mice by a Recombinant Vaccine Candidate Containing a Broadly Cross-Neutralizing Epitope within the VP2 EF Loop

Longfa Xu^{1,2*}, Delei He^{1,2*}, Zhiqun Li¹, Jun Zheng¹, Lisheng Yang¹, Miao Yu², Hai Yu^{1,2}, Yixin Chen^{1,2}, Yuqiong Que^{1,2}, James Wai Kuo Shih^{1,2}, Gang Liu², Jun Zhang^{1,2}, Qinjian Zhao^{1,2}, Tong Cheng^{1,2}, Ning-shao Xia^{1,2}

1. State Key Laboratory of Molecular Vaccinology and Molecular Diagnostics, School of Life Sciences, Xiamen University, Xiamen Fujian, 361102, PR China
2. National Institute of Diagnostics and Vaccine Development in infectious diseases, School of Public Health, Xiamen University, Xiamen Fujian, 361102, PR China

* Equally contributing authors

✉ Corresponding author: Tong Cheng. State Key Laboratory of Molecular Vaccinology and Molecular Diagnostics, Xiamen University, Xiamen 361102, China. Phone: 86-592-2184113; Fax: 86-592-2181258; E-mail: tcheng@xmu.edu.cn

© Ivyspring International Publisher. This is an open-access article distributed under the terms of the Creative Commons License (<http://creativecommons.org/licenses/by-nc-nd/3.0/>). Reproduction is permitted for personal, noncommercial use, provided that the article is in whole, unmodified, and properly cited.

Received: 2013.08.21; Accepted: 2013.12.25; Published: 2014.02.18

Abstract

Human enterovirus 71 (EV71) is the main causative agent of hand, foot, and mouth disease (HFMD) and is associated with several severe neurological complications in the Asia-Pacific region. Here, we evaluated that while passive transfer of neutralizing monoclonal antibody (nMAb) against the VP2 protein protect against lethal EV71 infection in BALB/c mice. Protective nMAb were mapped to residues 141-155 of VP2 by peptide ELISA. High-resolution structural analysis showed that the epitope is part of the VP2 EF loop, which is the “puff” region that forms the “southern rim” of the canyon. Moreover, a three-dimensional structural characterization for the puff region with prior neutralizing epitopes and receptor-binding sites that can serve to inform vaccine strategies. Interestingly, using hepatitis B virus core protein (HBc) as a carrier, we demonstrated that the cross-neutralizing EV71 antibodies were induced, and the VP2 epitope immunized mice serum also conferred 100% *in vivo* passive protection. The mechanism of *in vivo* protection conferred by VP2 nMAb is in part attributed to the *in vitro* neutralizing titer and ability to bind authentic viral particles. Importantly, the anti-VP2(aa141-155) antibodies could inhibit the binding of human serum to EV71 virions showed that the VP2 epitope is immunodominant. Collectively, our results suggest that a broad-spectrum vaccine strategy targeting the high-affinity epitope of VP2 EF loop may elicits effective immune responses against EV71 infection.

Key words: Human enterovirus 71, cross-neutralizing linear epitope, VP2 EF loop, therapeutic antibodies, epitope peptide vaccine.

Introduction

Human enterovirus 71 (EV71) is a viral pathogen within the Picornaviridae family and is one of the common causative agents of hand, foot and mouth

disease (HFMD)[1, 2]. EV71 infection can also lead to severe neurological complications such as aseptic meningitis, poliomyelitis-like paralysis, and possibly

acute encephalitis. A significant increase in EV71 epidemics with morbidity and mortality has been reported worldwide, especially in the Asia-Pacific region[3-5]. EV71-associated cases with high mortality rates of severe neurological diseases have been reported in Bulgaria in 1975, Hungary in 1978, Malaysia in 1997, Taiwan in 1998, 2000 and 2001, Australia in 1999, Singapore in 2000 and China in 2008[6-10]. In 2011 and 2012, there have been 1.61 million (including 509 deaths) and 2.19 million (including 569 deaths), respectively, reported by the Chinese Ministry of Health. In fact, EV71 is now represented a pre-eminent neurotropic enterovirus and a threat to global public health ever since the almost complete eradication of poliovirus.

EV71 is a small, non-enveloped, positive-stranded RNA virus, comprising four capsid proteins VP1, VP2, VP3 and VP4. High-resolution structural analysis of the mature virus and expanded natural empty particles shows that the EV71 virion is structurally similar to other enteroviruses, which has quasi-T=3 symmetry with 60 copies of each of the viral structural proteins VP1-VP3 that have β -sandwich "jelly-roll" folds; VP4 is located on the inner surface of the capsid. The EV71 virion, like other enterovirus, has a deep depression in the viral surface called the "canyon" and thought to be the receptor-binding site[11, 12]. On the outside of the particle, the loops exposed on the virion surface are important neutralizing immunogenic sites[13], residues 208-222 (GH loop) of VP1 being the most exposed are part of an important neutralizing epitope of EV71[14]. In addition, the residues 141-150 of VP2 was identified as an EV71 neutralization epitope by Liu *et al.*[15]. Interestingly, a large and highly variable surface loop of VP2 protein, referred to as the puff region, is also known to be a major neutralization site in other picornavirus including poliovirus, coxsackievirus and rhinovirus. For example, the neutralization site N-Ag II of poliovirus type 1 (PV1) is located in the EF loop and the carboxyl terminus of VP2[16]. The epitopes identified in coxsackie A9 (CAV9) also present in the "puff" region of VP2 as compared with poliovirus site N-Ag II[17]. Notably, this epitope lies in the protruding hydrophilic loop region exposed on the viral capsid surface, which is essential for understanding the mechanisms of virus uncoating and infection. It has been observed that the propeller tip and two-fold axes position, using the cryo-EM structures of poliovirus particles, are the site of egress of the N terminus of VP1 and of the viral RNA. The propeller tip is formed by the EF loop of VP2 and flanking polypeptide sequences from VP1 and VP3[18, 19]. Nevertheless, it has not been reported yet whether the EF loop of VP2 plays an important role in the dynamic EV71

cell-entry process.

Currently, no effective commercial antiviral therapies or prophylactic vaccines are available to combat EV71 infections. The prevention and control of EV71 has simply relied on public health surveillance and quarantine. Epitope peptides are considered promising candidates for new-generation vaccines as a well-defined immunogenic epitope can stimulate an effective and specific protective immune response while avoiding potential undesirable effects[20]. Moreover, by combining with multiple epitopes, it may be capable of developing a broad-spectrum vaccine to prevent a variety of viruses posing serious threats to health. Notably, containing a neutralizing epitope can serve as a promising vaccine as it can elicit specific antibodies inhibiting the interaction between the viral capsid protein and its cellular receptor[14]. Foo *et al.*[21] have identified the human CD4⁺ T-cell epitopes within VP1 capsid protein of EV71 that can induce proliferation of CD4⁺ T cells, then producing abundant IL-2 and IFN- γ upon stimulation. EV71-neutralizing antibodies elicited by the synthetic peptide SP70 were able to confer good *in vivo* passive protection against homologous and heterologous EV71 strains in suckling BALB/c mice[22]. Thus, epitope peptide vaccine is considered a promising candidate for EV71 prevention and infection treatment. While the VP2 EF loop (residues 136-150) are part of a neutralizing epitope of EV71, the epitope has failed to elicit virus neutralizing antibody response in mice[15, 23]. Therefore, the VP2 epitope remains a lack of deeper evaluation of the *in vivo* protection. In view of this, we are interested in developing a combination epitope peptide vaccine that possesses neutralizing ability against all EV71 genotypes, to facilitate the study of potential applications for prevention and infection treatment.

In this study, we generated an EV71-specific neutralizing monoclonal antibody (nMAb) (designated nMAb BB1A5) by immunization with activated whole virus of EV71 strain 52-3 (Genotype C4). The anti-VP2 MAb (BB1A5) protected mice against lethal EV71 infection. Then the nMAb was fully mapped, and found to target the cross-neutralizing linear epitope on VP2 capsid protein, spanning amino acids 141-155. In particular, combining with the high-resolution structures of EV71, we described that the neutralizing epitope lies in a large and highly variable surface loop of the VP2 protein, which plays important role during EV71 uncoating and infection. We generated a fusion protein with 149 aa of HBc protein and VP2-epitope, and confirmed this protein was able to spontaneously assemble into chimeric HBc particles by electron microscopy. We further proved that these particles were able to induce high

titers of VP2-epitope specific serum antibodies, and cross-neutralizing activity in cell culture. Consistently, it conferred 100% *in vivo* passive protection in suckling BALB/c mice against EV71 infection. Our results suggest that HBc particles carrying the cross-neutralizing epitope of VP2 could be a promising candidate to develop a broad-spectrum vaccine against EV71.

Materials and Methods

Cell lines, media and viruses.

RD cells were obtained from American Type Culture Collection (ATCC), cultivated in Minimal Essential Medium (GIBCO) supplemented with 10% FBS (PAA) plus 2mM L-glutamine, 100U of penicillin, and 100 µg of streptomycin per ml, and used for preparation of EV71 and other enterovirus strains, titration of those viruses, and neutralization assays. Those EV71 strains were respectively isolated from throat swabs and anal swabs of HFMD patients from the Jiangsu, Taiwan and Academy of Military Medical Sciences (Table 2). The EV71 virions were loaded onto a 15-50% continuous sucrose gradient, which resulted in fractions with densities at 20-40% after 3 h ultracentrifugation (32,000 × g, SW41Ti rotor, Beckman). The fractions were collected, and pelleted (100,000 × g for 2 h), resuspended in PBS. The purified virus was measured for the protein content using the BCA protein assay (Bio-Rad), and was stored in a -80°C freezer.

Serially diluted virus samples (from 10⁻¹ to 10⁻¹⁰) were added to RD cells in 96-well plates, and four wells were used at each dilution. The 96-well plates were incubated for 7 days at 37°C, 5% CO₂ and cytopathic effects (CPE) was observed using an inverted microscope. The 50% tissue culture infectious doses (TCID₅₀) values were measured by determining CPE and calculated according to the Behrens-Kärber method.

Monoclonal antibodies.

Anti-EV71 specific antibodies were produced by our laboratory. A group of 6 Female BALB/c mice (6-8 weeks) were immunized subcutaneously with activated EV71 strain 52-3 (10⁴ to 10⁵ TCID₅₀) emulsified in Freund's complete adjuvant. Two booster doses with the same 50% emulsion with Freund's incomplete adjuvant were delivered to the mice at two-week interval. The same antigen in PBS was directly injected into spleen of mice with the highest serum antibody titers against immunogen 3 days prior to cell fusion. The fusion of spleen cells with mouse myeloma cell was done as described[24]. Fusion of splenocytes with Sp2/0Ag-14 myeloma cells (University of Pavia, Lombardy, Italy) was performed using meth-

ods described in detail elsewhere[24, 25], with some modifications. Briefly, hybridomas were selected with GiBCO RPMI1640 plus hypoxanthine-aminopterin-thymidine and 20% fetal bovine sera, and supernatants were screened by indirect ELISA or neutralizing test against EV71. Positive clones were further grown in GiBCO RPMI1640 plus 10% FBS for colonial separation. Stable cell lines capable of producing monoclonal antibodies were cultured first using 24-well plates, and then by 100ml cell culture flask for further amplification. Cells collected from the cell flask were injected into a mouse abdominal cavity. Ascitic fluid was extracted from the mouse after 7-10 days. Purified MAbs were got from ascitic fluid by precipitating with 50% ammonium sulfate, dialyzing with phosphate buffer (PB) at pH 7.4 and purifying with DEAE column by HPLC. EV71-specific monoclonal antibodies were conjugated with horseradish peroxidase (HRP) by the NaIO₄ oxidation method followed by gel filtration chromatography on a Superdex 200HR column. The purified antibodies were saved at -20°C.

Production of recombinant proteins. (i) Recombinant EV71 viral proteins.

Viral RNA was extracted from the culture supernatant of the EV71 strain 52-3 infected cells using Trizol reagent (Invitrogen). The cDNA was synthesized using Superscript III reverse transcriptase (Invitrogen) with three sets of reverse primers (Table 3). The purified PCR products were restricted by Nde I and Xho I enzymes (TaKaRa, Japan) and cloned into the pTO-T7 plasmid vector[26]. The recombinant plasmids were verified by sequencing. For cloning and expression experiments, E.coli strains DH5α and ER2566 (NEB, American) were used. The plasmids to express recombinant VP proteins were transformed into E.coli ER2566. After 6 h of induction with 0.2 mM isopropylthio-β-D-galactopyranoside (IPTG) at 37°C, cells were centrifuged (9,000 × g for 5 min) and collected in buffer (20 mM Tris-HCl, 5 mM EDTA, 50 mM NaCl, pH 8.0) prior to SDS-PAGE and western blotting analysis. The recombinant EV71 viral proteins were purified by electroelution combined with SDS-PAGE. The concentrations of each of the recombinant EV71 antigens were determined using a BCA protein assay, and antigens were saved at -20°C.

(ii) HBc(aa1-149) and HBc-VP2(aa141-155).

To express the HBc-VP2(aa141-155) fusion protein, the VP2(aa141-155) gene was inserted into the pC149/mut plasmid vector[27] by anneal oligos to generate a plasmid HBc-VP2(aa141-155) with the primers (Table 3), which inserted 15 amino acids between aa 78 and 83 of pC149/mut. Assemble the annealing reaction by mixing 1 µL of each oligo with 48

μ L annealing buffer (100 mM NaCl and 50 mM HEPES pH 7.4), Incubate the mixture at 90°C for 4 min, and then at 70°C for 10 min. Slowly cool the annealed oligos to 10°C. The annealed oligo inserts can be used immediately in a ligation reaction. Recombinant HBc-VP2(aa141-155) and pC149/mut were prepared as described previously[27]. Finally, the proteins were determined by high performance liquid chromatogram (HPLC) (System Gold Nouveau, Beckman Coulter Ins.) assay.

SDS-PAGE analysis and Western blotting.

The purified recombinant proteins were analyzed by 12% SDS-PAGE and were stained by Coomassie blue. For Western blotting, mouse monoclonal anti-HBc antibody (Beijing Wantai Biological Medicine Co.) and nMAb BB1A5 were used. Briefly, the transferred nitrocellulose membrane was incubated in blocking solution (5% skim milk in Tris-buffered saline, TBS) for 1 h at 37°C, and washed thrice with TTBS (0.05% Tween 20 in TBS) followed by incubation at 37°C for 1 h with anti-HBc or nMAb BB1A5 that was prediluted to 1:1,000 with blocking solution, and washed thrice times with TTBS. Protein bands were reacted in turn with MAb diluted 1:5,000 followed by alkaline phosphatase (AKP)-conjugated goat anti-mouse IgG (DAKO) and then developed with bromochloroindole phosphate/nitro blue tetrazolium substrate (BCIP/NBT).

Electron microscopy.

The fusion protein HBc-VP2(aa141-155) and HBc(aa1-149) were analyzed by negative staining electron microscopy. Briefly, Samples were absorbed onto a 200 mesh carbon-coated copper grids for 5 min. Then the grids were washed twice with ddH₂O and air-dried. Specimens were evaluated by JEM-2100HC electron microscope (JEOL, Tokyo, Japan) at about 25,000 magnification.

In vitro neutralization assay.

RD cell monolayers were prepared at 400,000 cells/ml in MEM (GIBCO) supplemented with 10% FBS (PAA) and seeded at 40,000 cells per well into 96 well plates (NUNC). Serum samples were heat-inactivated at 56°C for 30 min. Two-fold serial dilutions from 1:8 to 1:2,048 were prepared in virus diluent (MEM). Each sample was challenged with 100 TCID₅₀ per well of the EV71 strain 52-3. We also used other five EV71 subgenotype strains (Table 2). After incubated at 37°C, 5% CO₂ for 1 h, the serially diluted samples were incubated with RD cells prepared in 96 well plates. The cultures in the 96-well plates were incubated at 37°C for 7 days, and the TCID₅₀ values were measured by CPE in infected cells. The neutralization titers were read as the highest dilution in over

50% CPE, taken as the average of the triplicates.

Design and synthesis of peptides.

The entire VP2 capsid protein of EV71 strain 52-3 was used as a template to synthesize overlapping 15-mer peptides at MMG Co. (Germany). Each peptide contains 15 amino acid residues with 10 residues overlapping with the neighboring peptides. The VP2 epitope (residues 136-155) was synthesized to contain a single alanine substitutions at each amino acid position to identify key binding residues recognized by BB1A5.

ELISA. The 96-well plates were coated at 4°C overnight with 1 μ g/well of Peptides, HBc(aa1-149), HBc-VP2(aa141-155) and rVP2 in 50 mM carbonate buffer (pH9.6). After washed with PBS containing 0.05% Tween 20, the plates were blocked with 0.05% Tween 20 and 1% bovine serum albumin in PBS for 2 h at 37°C. The nMAb BB1A5 to peptides (1:1,000), the serum samples using 10-fold dilution series, and the first dilution was 100-fold, added to the wells, and were applied for 30 min at 37°C. Horseradish peroxidase-conjugated goat anti-mouse (GAM-HRP) IgG antibody was added into each well in a 1:5,000 dilution, and incubated for 30 min at 37°C. Visualization was done by incubation with o-phenyl-diamine-2HCl (10 μ g/mL in 5 mM Tris-HCl, pH7.0) for 15 min, and the reaction was stopped by adding 50 μ L of 2 M H₂SO₄. The wells were washed 5 times with PBST (0.05% Tween 20 in PBS) between each step. Absorption was measured at A_{450/620}. The procedure adopted in virus ELISA is the same as given in peptides and recombinant antigens ELISA. The procedure adopted in virus ELISA and competitive ELISA is the same as given in peptides and recombinant antigens ELISA. For competitive ELISA, nMAb BB1A5 (10 or 50 μ g/well), the serum of mice immunized with HBc-VP2(aa141-155) and HBc(aa1-149) (1:20 dilution) were added to the wells in blocking solution (final volume: 50 μ L/well), and incubated for 30 min at 37°C. Then the human serum (1:50 dilution) was added and incubated at 37°C for 30 min. After the washings, mouse anti-human antibody labeled with horseradish peroxidase was added to the plates (100 μ L/well) at 1:200 dilution in PBS with 1% BSA (bovine serum albumin), and incubated for 30 min at 37°C. The OD value was converted to percentage inhibition (PI) using the formula: PI (%) = 100 - [(OD_{sample}/OD_{control}) × 100]. Where OD of control well represents the well containing human serum alone.

Immunofluorescence Assay (IFA)

RD cells were plated onto 13×13 mm glass coverslips in 24-well plates and then infected with EV71

strain JS 52-3. After 12 h cells on the cover glasses were fixed with 4% paraformaldehyde for 30 min, permeabilized with PBST (PBS+0.3% Triton X-100) for 10 min and blocked for 1 h with goat serum. Fixed and permeabilized cells were incubated with nMAb BB1A5 (1 µg/ml) and HBC-VP2(aa141-155) antisera (1:200 dilution). After 1 h of incubation at 37°C, cells were washed and incubated with GAM-FITC for 30 min. Finally, after 5 min DAPI nuclear staining, cells on the cover glasses were observed using confocal microscopy (MRC-1024, Biorad, Hercules, CA).

Capture ELISA and quantitative real-time RT-PCR.

Serial dilutions of JS 52-3 with initial concentration of 10^7 TCID₅₀ were captured by antibody (2 µg/well) coated on microplate and incubated at 37°C for 2 h. After washings, Viral RNA was extracted using a QIAamp Mini viral RNA Extraction Kit (Qiagen). All samples were subject to quantification for viral RNA copies by real-time RT-PCR, as described previously [28, 29]. An unrelated antibody was used as negative control. The viral copies of EV71 genome was indirectly quantified from a DNA plasmid standard curve by using EV71-VP1. Generation of a standard curve and the log₁₀ values of the viral RNA copies/ml were analyzed by using the CFX manager software (Bio-Rad Laboratories, Inc.).

Clinical human serum samples

The clinical human serum samples used for this study were well-characterized samples obtained from previous study protocols [28]. Each serum sample was divided into two aliquots prior to testing. One aliquot was used to detect the viral RNA by RT-PCR. Another aliquot was used to detect EV71 specific neutralizing antibody titer (Table 4). All serum samples were kept in aliquots at -20°C until use.

Mice immunization.

For immunization, five female Special pathogen free (SPF) BALB/c mice (6-8 weeks) per group were immunized subcutaneously (s.c.) with a 50% emulsion of Freund's complete adjuvant containing either 100 µg of conjugated recombinant proteins HBC-VP2(aa141-155) or HBC(aa1-149). Three booster doses in 50% emulsions with Freund's incomplete adjuvant were given at two weekly intervals. The immunized animals were bled at 0, 2, 4, 6, 8, 10, 12 weeks for the serological tests, and the serum was collected and stored at -80°C.

Passive protection test in mice.

Inbred BALB/c mice were obtained from the Slac Laboratory Animal Co., Ltd., Shanghai, China. All institutional guidelines for animal care and use

were strictly followed throughout the experiments. Groups of mice (n=11~13) within day 1 after birth were challenged with 50 µL of EV71 (10^7 TCID₅₀ per mouse) intraperitoneally (i.p.). For sera protection, 50 µL of mice HBC-VP2(aa141-155) immunized sera were administered i.p. 24 h later, suckling mice from control groups were given HBC(aa1-149) immunized sera. For antibody treatment, 50 µL of nMAb (BB1A5) was injected i.p. 24h later at a concentration of 60 µg per body weight (g), suckling mice from control groups were given 50 µL of MAb (EV71-X4G1) and PBS. Every group contained two independent experiments. Mice were monitored daily for body weight, clinical illness and death until day 20 post-infection. The grade of clinical disease was scored as follows: 0, healthy; 1, lethargy and inactivity; 2, wasting; 3, limb weakness; 4, hindlimb paralysis; and 5, moribund and death. The protected mice were healthy throughout the experiments.

Histopathologic and immunohistochemical staining.

At day 5 to day 8 post-infection, challenged mouse were subjected to histopathologic and immunohistochemical examination. Brain, spine, heart, liver, lung, intestines and limb skeletal muscles were separately harvested after euthanization, and then fixed by immersion in 4% PBS-buffered formalin for at least 72 h at room temperature. Fixed tissues were bisected, embedded in paraffin and sectioned on 4 mm thick. For histopathologic test, tissue sections were stained with hematoxylin and eosin. Immunohistochemical examination was performed by using Ultrasensitive TMS-P kit (Fuzhou Maixin Biotechnology Development Co., Ltd., Fuzhou, China) and DAB Detection Kit (Streptavidin-Biotin; Fuzhou Maixin Biotechnology Development Co., Ltd., Fuzhou, China) according to manufacturer's recommendation. The primary antibody, I2D7, was a mouse anti-EV71 VP1 monoclonal antibody (1 mg/mL, 1:1,000 dilution).

Results

Neutralizing MAb against the VP2 protein protect mice from EV71 infection.

We assessed the neutralizing (BB1A5) MAb which reacted specifically with rVP0 and rVP2 antigens, and did not cross-react with other capsids (Fig. 1A, B). The in-house developed BB1A5 was found to have a cross-genotype neutralizing ability against EV71 strains of the B3, B4, C2 and C5 subgenotypes with titers of 1:32 respectively. The *in vivo* protection ability was evaluated by a mouse model of EV71 infection using a mouse-adapted EV71 strain

pSVA-MP4, with which newborn BALB/c mouse infected intraperitoneally (10^7 TCID₅₀) were found to have neurological manifestations such as limb weakness and limb paralysis prior to death. BB1A5 was administered intraperitoneally (60 µg/g) respectively 24 hours after challenging. Excitingly, passive transfer of neutralizing (BB1A5 [IgG2a]) provided significant protection (100% [$P < 0.0001$]) by contrast to PBS treated mice (8%). The MAb EV71-X4G1 was a negative control, which showed a 8% protection rate (Table 1). Being able to react with the rVP2 protein and *in vitro* neutralization assay imply that the VP2 antigen contains a cross-genotype neutralization epitope.

TABLE I. MAb protection of newborn BALB/c mice^a

MAb or control	Isotype	Neutralizing titer	Survival(%)	P value
PBS		0	1/13 (8)	
BB1A5	IgG2a	32	13/13 (100)	<0.0001
X4G1	IgG2b	< 8	1/13 (8)	

^aNewborn BALB/c mice was infected with 10^7 TCID₅₀ of pSVA-MP4 as described above, then the indicated MAbs(60 µg/g) were passively injected i.p. 24 hours later. Survival survey was followed for 20 days, and P values were analyzed by the log-rank test versus results for PBS-treated mice.

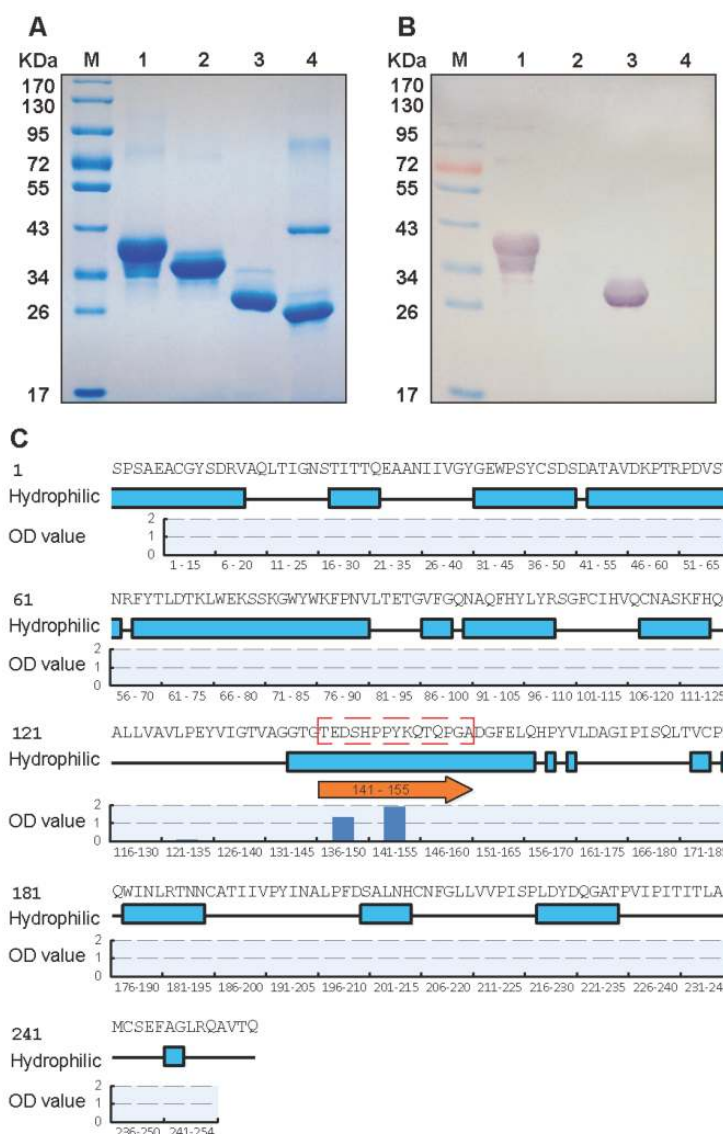


Fig. 1. Specificity of nMAb BB1A5 to EV71 antigens. (A) SDS-PAGE analysis of purified EV71 antigens. **(B)** Western blotting with EV71-specific nMAb BB1A5. The amount of viral proteins loaded in each lane was 10 µg. The lanes are as follows: lane M, molecular mass marker; lane 1, non-fusion VP0 recombinant protein (36 kDa); lane 2, non-fusion VP1 recombinant protein (33 kDa); lane 3, non-fusion VP2 recombinant protein (28 kDa); lane 4, non-fusion VP3 recombinant protein (27 kDa). **(C)** Identification of neutralization epitopes in the VP2 capsid protein by peptide ELISA. A set of 49 overlapping peptides covering the entire sequences of VP2 (49×15-mer peptides) were used to coat 96-well plates. Hydrophobicity plots were generated using the Kyte-Doolittle algorithm implemented in Protean (Lasergene, DNASTar Inc., Madison, WI). The VP2-epitope (peptide aa141-155) is indicated on the plot.

In vitro characterization of protective MAb.

A set of 49 synthetic peptides consisting of 15 amino acids in length spanning the entire VP2 capsid protein of EV71 strain 52-3 was prepared for epitope mapping by peptide ELISA as described in Materials and Methods. Among these 49 peptides, MAb (BB1A5) only reacted with peptides corresponding to residues 136-155 of the VP2 subunit (Fig. 1C) which was also identified as an EV71 neutralization epitope by Liu *et al.* [15]. In contrast, anti-VP2 MAb was observed to have higher reactivity with peptides aa141-155 than aa136-150. The Kyte and Doolittle hydrophobicity plots of the VP2 capsid protein indicated that aa141-155 is located within the major hydrophilic regions of the protein (Fig. 1C). Therefore it is likely to be in a surface-exposed region. Taken together, these results reveal that there is a linear cross-genotype neutralization epitope located within residues 141-155 of VP2. To identify critical amino acid residues within the binding of BB1A5 to VP2 epitope, alanine (Ala) substitution studies were performed. The results presented in Fig. 2 show that the mutation of Thr (T141A), Glu (E142A), Ser (S144A) and His (H145A) significantly affected the binding affinity, suggesting that these residues are the most critical antigenic determinants of the VP2 epitope.

Structural analysis of the cross-neutralizing epitope of VP2.

The structural studies of epitopes can provide useful insights into their properties, including antigenicity and factors contributing to neutralizing activity. Recently, Wang *et al.*[11] have determined a high-resolution crystal structures of EV71 (genotype

C4), including the 150S mature virion at 2.3-Å resolution (Fig. 3A) and an expanded form of 82S empty assembly intermediate at 2.88-Å resolution (Fig. 3B). Through atomic-level descriptions of two different conformational states of the virus, Wang *et al.*[11] have proposed a model for enterovirus uncoating in which the GH loop of VP1 acts as an adaptor-sensor for cellular receptor attachment. As shown in Fig. 3D, the process of expansion results in the appearance of a large hole (8×25 Å) at the two-fold axis, disrupting the pair of VP2 α A helices, and a second hole (7×9 Å in size) at the base of the canyon, either of which might allow egress of the N terminus of VP1 and of the viral RNA. Notably, the cross-neutralizing epitope lies in the EF loop (magentas in Fig. 3C), the most prominent and highly variable surface loop of the VP2 protein is the “puff” region that forms the “southern rim” of the canyon. As shown in Fig. 3C,D, a separation similar to that on the VP2 α A helices at the two-fold axes is observed on the pair of VP2 EF loops, where C α movements reach ~ 4.4 Å. What's more, the VP2 epitope undergoes a major conformational switch, with residues 148–152 converting from helix to loop upon expansion, and the Lys149 side chains reposition to induce the conformational rearrangement (Fig. 3E,F). Interestingly, the VP2 epitope near the GH loop of VP1 (marine in Fig. 3C) interacts with the GH loop of VP3 from a neighboring protomer (firebrick in Fig. 3C), and these epitopes lie in the area surrounding the second hole. Taken together, the structural characterization of the EF loop of VP2 reveals features that may provide useful insights into the trigger for the conformational changes associated with the EV71 uncoating and infection.

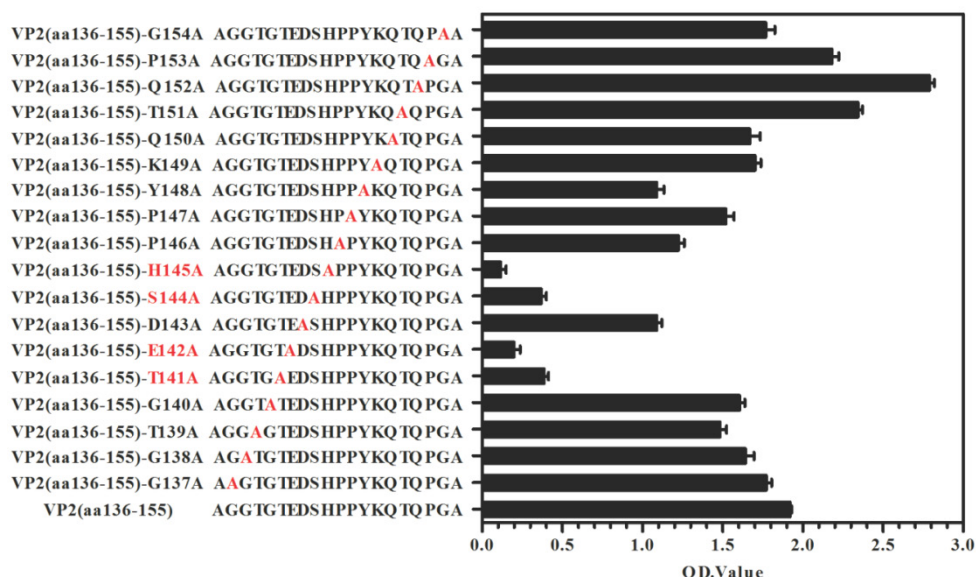


Fig. 2 Identification of antigenic key residue(s) within VP2(aa136-155). Ala scanning (i.e., the substitution of alanine residues (A) for amino acids within the epitope) were used to determine key amino acids for BB1A5 binding. The binding affinity was measured by peptide-ELISA. Error bars indicate standard error of mean from three individual experiments.

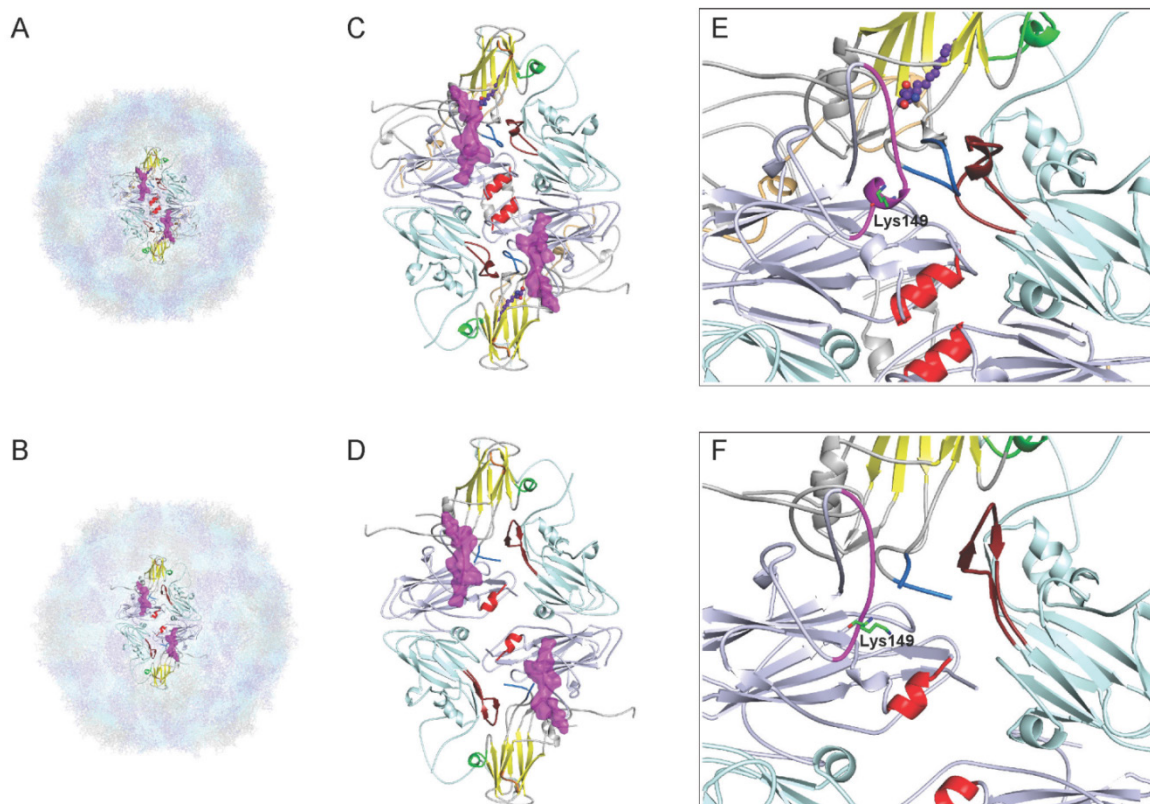


Fig. 3. Comparison of the cross-neutralizing epitope of VP2 from the mature virion and the expanded particle of Wang et al. [11]. (A) The mature EV71 virion (PDB: 3VBS), VP1, VP2, VP3 and VP4 are drawn in gray, lightblue, lightcyan and lightorange, respectively. (B) The expanded empty capsid (PDB: 3VBU), consisting of VP0 (a precursor protein in which VP4 and VP2 are covalently linked), VP1 and VP3. (C,D) Stereo pictures showing the VP2-epitope between the mature virus and empty particles and two holes in the expanded structure. The diamond-shaped dimers are bounded by two fivefold and two threefold axes. A two-fold axis is at the center of the diamond. The pocket factor (purple) is shown as a model of sphingosine and present in VP1. The VP1 β -barrel, BC loop and surrounding residues 163-177 of VP1 from the "northern" rim of the canyon are indicated by yellow, orange, and green, respectively. The cross-neutralizing epitope of VP2 is shown in magentas on the canyon region, together with the GH loop of VP1 (marine) and VP3 (firebrick), lies in the area surrounding the second hole. The pair of VP2 α A helices at the two-fold axis are shown in red. (E,F) Note the large conformational rearrangement in the Lys149 side chains of VP2-epitope. C, E, mature virus; D, F, expanded particle. All models were prepared with PyMOL (DeLano Scientific).

Insertion of the cross-neutralizing linear epitope of EV71 VP2 into HBc protein.

We used a carboxyl-terminally truncated HBc protein (aa1-149) as an immune-enhancing carrier protein to present the linear cross-genotype neutralization epitope VP2(aa141-155) as a foreign antigen. The VP2(aa141-155) gene sequence was inserted into the DNA sequence that codes for the major immunodominant region (MIR) of HBc(aa1-149). The resulting HBc-VP2(aa141-155) fusion protein was efficiently synthesized in *E. coli* ER2566. As shown in Fig. 4A, densitometric scanning of Coomassie blue stained gels revealed that the purified fusion protein HBc-VP2(aa141-155) amounted to more than 95% of the total protein present, which was sufficiently pure for immunizations. A band of identical mobility was detected by Western blotting using mAbs against HBc(aa1-149) and HBc-VP2(aa141-155) (Fig. 4B,C). Direct confirmation of efficient particle formation was obtained by negative staining electron microscopy (EM). Numerous empty core-like particles with an average diameter of 30 nm were observed (Fig. 4D,E). The morphology of the chimeric HBc-VP2(aa141-155)

particles did not differ significantly from that of the particles formed by HBc(aa1-149) protein without insertion.

Immunization of animals with HBc-VP2(aa141-155) particles presenting VP2-epitope.

To investigate the immunogenicity of chimeric HBc particles, we immunized mice with HBc-VP2(aa141-155) and HBc(aa1-149), respectively, using Freund's adjuvant. The mice were immunized at two-week intervals for four times. We analyzed the serum by ELISA to identify IgG antibodies directed against VP2, HBc-VP2(aa141-155) and the carrier protein HBc. After 2 weeks from the first immunization, anti-VP2 antibody was detectable in the serum of mice immunized with HBc-VP2(aa141-155), and at the fourth week the titer was around 10^5 , while in the serum of mice immunized with HBc(aa1-149) and adjuvant almost no anti-VP2 antibody was detectable (Fig. 5A). Since we used rVP2 as coated protein of the ELISA, the anti-VP2 titer actually was the representative of VP2 epitope specific antibodies in the sera of

HBc-VP2(aa141-155) immunized mice. So our result suggests that the chimeric HBc protein carrying a VP2 epitope can induce VP2-epitope specific antibodies in mice. We also compared the anti-HBc-VP2(aa141-155) antibodies in different groups (Fig. 5B). Obviously both HBc-VP2(aa141-155) and HBc(aa1-149) induced high titer of anti-HBc-VP2(aa141-155) antibodies (actually most of which should be anti-HBc(aa1-149) antibodies as shown in Fig. 5C).

The antisera were also analyzed by an *in vitro* neutralization assay to determine their ability to neutralize EV71 strain JS 52-3 replication in RD cells. The neutralization titers against EV71 were barely detectable (<1:8) in the anti-HBc(aa1-149) antisera. In a time-scale study (Fig. 6A), the HBc-VP2(aa141-155) antisera resulted in a neutralization titer profile similar to the antibody titer profile, with neutralization titers culminating at 8 weeks and persisting for at least 12 weeks. After four immunizations with adjuvant, the HBc-VP2(aa141-155) induced a neutralization titer of 1:32 against EV71 replication in RD cells. These antisera against homologous VP1 of the JS strain exhibited cross-neutralization activities against wild-type EV71 strains from subgenogroups B3, B4, C2, C4 and C5 (Table 2). The data showed that HBc-VP2(aa141-155) induced low neutralization antibody titers and had a potential to be effective against

heterologous EV71 subgenogroups. The neutralization titer of anti HBc-VP2(aa141-155) serum was around 1:32 and 1:64 against EV71 subgenotype strains (Fig. 6B). The antisera towards the VP2-epitope were also assayed by ELISA where the wild-type EV71 strains were individually coated onto the 96-well microtiter plates. A strong positive signal was obtained when antisera were incubated with the virus (Fig. 6C). Therefore, HBV core particles-surface displaying VP2-epitope successfully retained antigenic sites of EV71 and elicited neutralizing antibody responses and thus may serve as a candidate vaccine for EV71.

TABLE 2. The information of related enterovirus strains

Virus strain	Genotype	Origin	Year	Genbank No.
pSVA	EV71 B3	/	/	/
02203	EV71 B4	Taiwan CDC	2006	JF420549
03149	EV71 C2	Taiwan CDC	2008	JF420552
52-3	EV71 C4	Jiangsu CDC	2006	FJ600325
H8	EV71 C4	AMMS	2008	JF420580
02969	EV71 C5	Taiwan CDC	2008	JF420554

AMMS: Academy of Military Medical Sciences, China

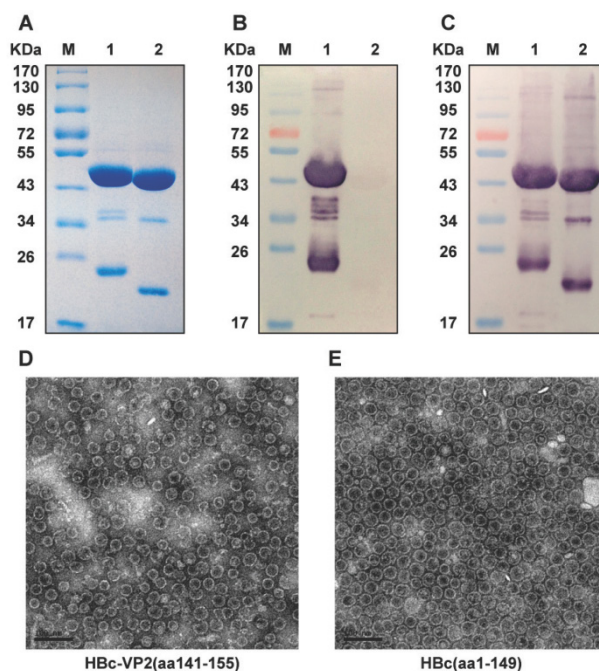


Fig. 4. Analysis of purified recombinant proteins HBc-VP2(aa141-155) and VLP formation. (A) SDS-PAGE analysis of purified recombinant proteins. Lane M, molecular mass marker; Lane 1: purified HBc-VP2(aa141-155); Lane 2: purified HBc(aa1-149). Western blotting with nMAb BB1A5 (B) and mouse monoclonal anti-HBc antibody (C). Electron microphotographs of HBc-VP2(aa141-155) (D) and HBc(aa1-149) (E) particles. Magnification: ×25K.

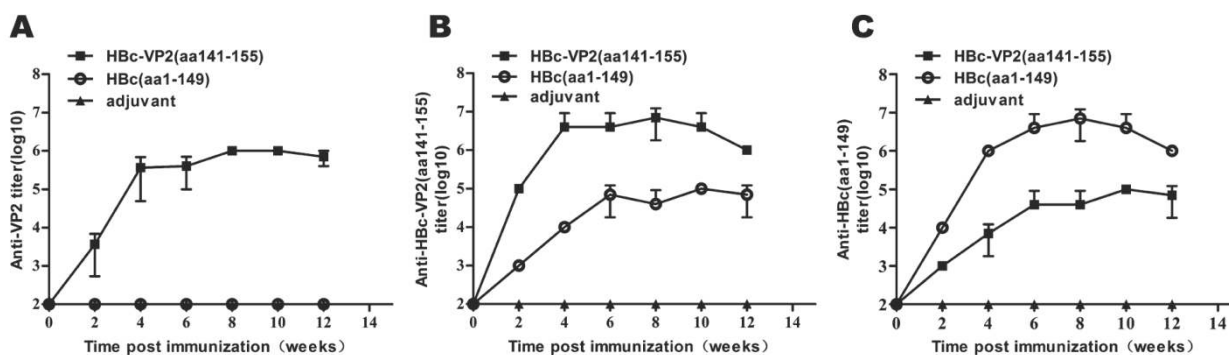


Fig. 5. Dynamic changes of antibody titer in immunized mice. Two groups of mice, each including 5 female BALB/c mice, were immunized subcutaneously with four injections of 100 µg of different recombinant proteins on weeks 0, 2, 4, 6 and were bled at 0, 2, 4, 6, 8, 10, and 12 for the serological tests. **(A)** rVP2 as coated protein to detect VP2-epitope specific antibodies; **(B)** HBC-VP2(aa141-155) as coated protein to detect anti-HBc(aa1-149) antibodies and VP2-epitope specific antibodies (for rVP2 group); **(C)** HBC(aa1-149) as coated protein as a control. Each point represents the mean reciprocal log₁₀ endpoint titers and standard error.

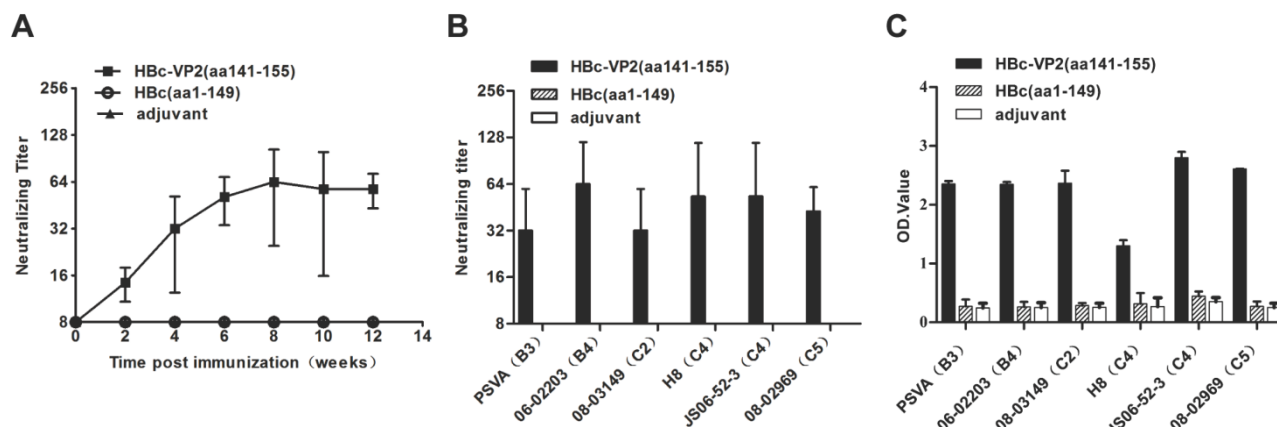


Fig. 6. Analysis of VP2-epitope specific neutralizing antibodies in immunized mice. EV71 neutralization titers of the antisera were determined by *in vitro* neutralization assay. Anti-EV71 IgG of antisera measured by ELISA using purified EV71 subgenotype strains as coating antigen. **(A)** Neutralizing antibodies in the sera of immunized BALB/c mice to EV71 strain JS 52-3 were tested. **(B)** Cross-Neutralization antibodies titers elicited by HBC-VP2(aa141-155) in mice at 8 post immunization weeks against 6 EV71 subgenotype strains. **(C)** Reactivity of antisera (1:500 dilution, 8 post immunization weeks) to wild-type EV71 strains.

High-affinity VP2 epitope immunized mice serum protect suckling mice from lethal EV71 strain infection.

The efficacy of passive protection of the antisera induced by the chimeric HBC-VP2(aa141-155) particles was evaluated by the EV71 mouse model described above. In the experiment, newborn suckling BALB/c mice was challenged with pSVA-MP4 (10⁷ TCID₅₀) followed by administering intraperitoneally with the respective antisera 24 hours later. Groups of mice that received the anti-HBC-VP2(aa141-155) antisera with an *in vitro* neutralizing titer of 1:32 did not display any symptoms and remained healthy until the end of the experiment. When the neutralizing antibody titer of HBC-VP2(aa141-155) antisera was reduced to 1:16, the survival rate of EV71-infected suckling mice dropped to 78% and subsequently to 58% when the neutralizing antibody titer was further reduced to 1:8. While groups of mice that received anti-HBC(aa1-149) antisera developed severe limb paralysis from day 5 post-infection (Fig. 7A) and reached to an average 4 score at day 7 post-infection (Fig. 7B). The final sur-

vival rate was 9.09% (Fig. 7C). To understand the distribution of virus and the pathological changes after i.p. inoculation, neonatal mouse with limb paralysis between day 5 and day 8 post-infection were selected to undertake hematoxylin and eosin (HE) stain and immunohistochemistry (IHC) examinations. Although both protected group (Fig. 8A) and mock group (Fig. 8B) showed positive stains in intestine, the situations in brain and limb muscle were quietly different. IHC results confirmed the presence of EV71-VP1 antigen in the medulla oblongata (Fig. 8C) and limb muscles (Fig. 8E). In comparison, no positive stain was found in the medulla oblongata (Fig. 8D) or limb muscles (Fig. 8F) from protected group. HE examination of mice from mock control revealed severe necrotizing myositis (Fig. 8G) in the limb muscle compared to normal morphous (Fig. 8H) from protected group. These results showed that HBC-VP2(aa141-155)-immunized serum was able to completely protect newborn mice against lethal EV71 challenge at an *in vitro* cross-neutralizing titer of 1:32.

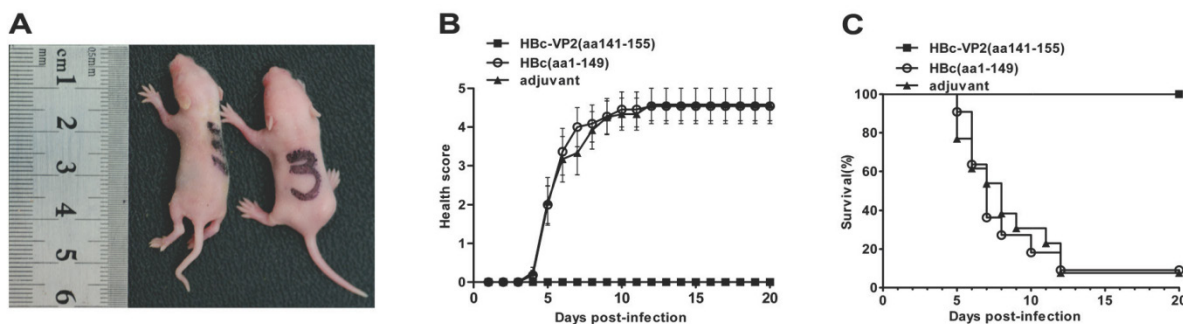
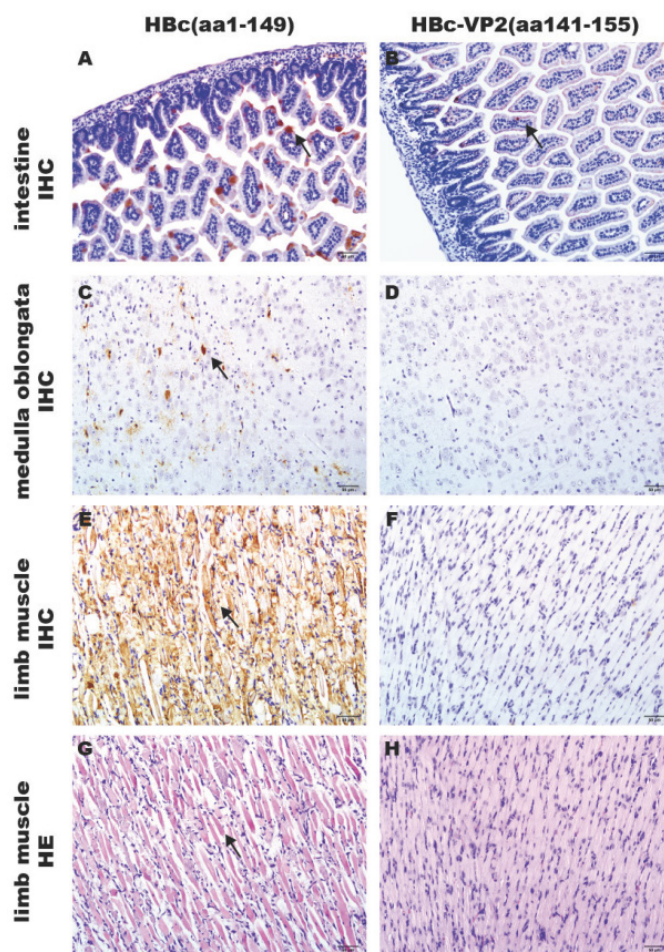


Fig. 7. In vivo passive protection by anti-HBc-VP2(aa141-155) antisera. Groups of one-day-old suckling BALB/c mice were infected i.p. with pSVA-MP4 (10^7 TCID₅₀ per mouse), then HBc(aa1-149)-immunized serum, HBc-VP2(aa141-155) immunized serum or adjuvant immunized serum was injected i.p. 24 h later. **(A)** Representative picture of hind limb paralysis caused by pSVA-MP4 at day 5 post-infection. The mouse on the right-hand side is an age-matched control from the HBc(aa1-149)-immunized group. **(B)** Health score of clinical disease and **(C)** mortality were monitored and recorded daily after infection. Representative results of two independent experiments were shown (n=11). The Log-rank (Mantel-Cox) test was used to compare the survival rates of mice between HBc(aa1-149) or adjuvant group and HBc-VP2(aa141-155) group at day 20 post-infection. ****p* < 0.0001.

Fig. 8. Contrast of pathological changes between HBc-VP2 (aa141-155)-immunized group and HBc(aa1-149)-immunized group. Groups of one-day-old BALB/c mice were inoculated i.p. with 10^7 TCID₅₀ pSVA-MP4 per mouse, 24 h later, 50 μ L HBc(aa1-149)-immunized serum or HBc-VP2(aa141-155)-immunized serum were injected i.p.. Mice were sacrificed and tissues were collected as described in Materials and Methods. Positive stains occurred in intestine of both groups **(A B, arrow)**. In protected group, positive stains were detected in the medulla oblongata **(C, arrow)** and limb muscle **(E, arrow)**, severe necrotizing myositis was distributed widely in the limb muscle **(G, arrow)**. In contrast, positive stain was absent in the medulla oblongata **(D)** and muscle **(F)** of adjuvant control, and no pathological changes were seen in the limb muscle **(H)**. Samples of A, B, C, D, E and F were processed by IHC analysis; Samples of G and H were stained with hematoxylin and eosin. Magnifications, $\times 200$.



Binding property of anti-VP2(aa141-155) and dominance in human serum.

We evaluated the VP2 neutralizing antibodies for their capacity to bind authentic EV71 virions. On the whole cell level, IFA was used to test the reactivity of nMAb BB1A5 and HBc-VP2(aa141-155) antisera with EV71 strain JS 52-3 infected RD cells. Consistently, the results showed that the VP2 antibodies had good reactivity with EV71 virus (Fig. 9A). In addition, Serial dilutions of JS 52-3 with initial concentration of 10^7 TCID₅₀ were captured by nMAb BB1A5. The dilution of 10^2 TCID₅₀ with a viral EV71 copy number of 59.84/ml still generated a detectable signal in the real-time PCR detection assay. Therefore, the nMAb BB1A5 also showed good reactivity with normal EV71 viral particles by capture ELISA(Fig. 9B). These data demonstrate that the anti-VP2(aa141-155) could bind normal EV71 virions, explaining its ability to inhibit virus attachment to cells. In addition, eight human serum samples from patients with EV71 were positive for PCR detection and neutralization assay (Table 4). To investigate the abundance of VP2 epitope in human serum, we performed competitive ELISA experiments. As seen in Fig. 9C, HBc-VP2(aa141-155) antisera exhibited 61% inhibition (*P*<0.05) by calculat-

ing the mean PI value, while the HBc(aa1-149) antisera showed 30% inhibition. Neutralizing (BB1A5 [IgG2a]) MAbs provided significant inhibition (61% [*P*<0.05]) by contrast to nonrelated monoclonal antibody (40%). The anti-VP2 MAbs have been shown to block more than 60% of (EV71-infected) human sera from binding EV71 virus 52-3, thus VP2 epitope is immunodominant in human and seen as critical for eliciting a neutralizing EV71 response. The clinical human

serum samples were also assayed by ELISA where the VP2 epitope and EV71 strain JS 52-3 were individually coated onto the 96-well microtiter plates. A strong

positive signal was obtained when human serum were incubated with VP2(aa141-155) epitope (Fig. 9D).

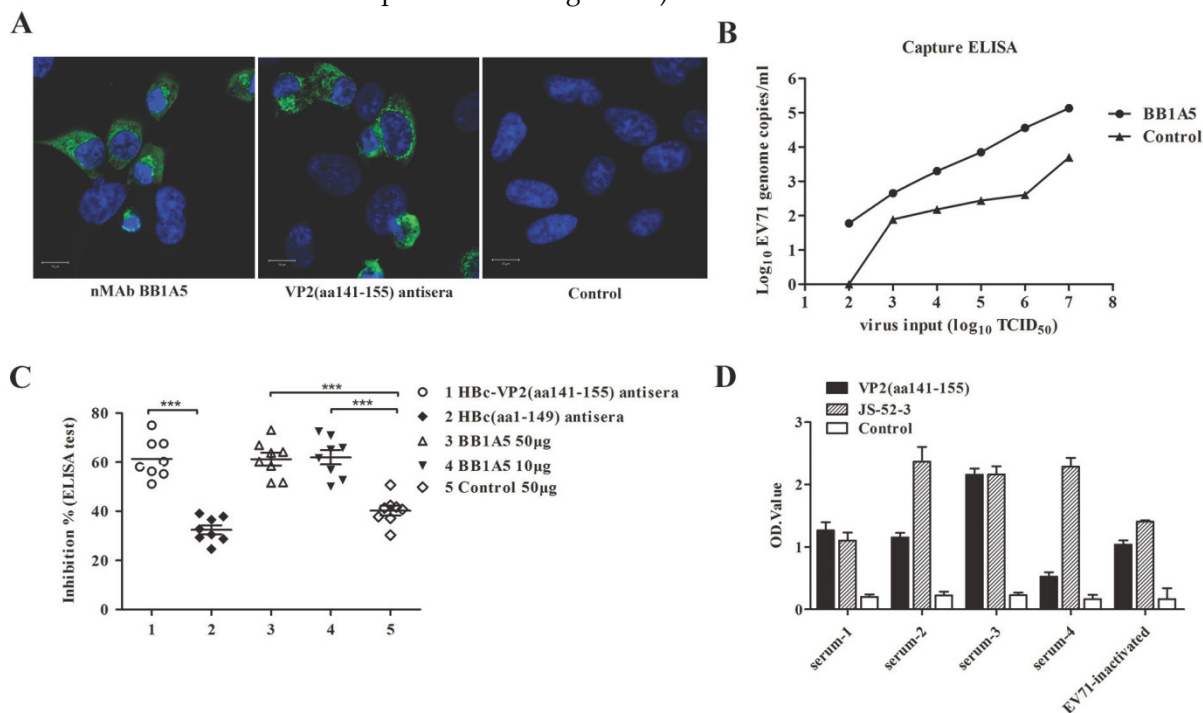


Fig. 9. Analysis of the affinity of VP2 nMAb against authentic EV71 particles and dominance in human serum. (A) Immunofluorescence assay of JS 52-3 infected RD cells. (B) The number of RNA genome copies/ml determined by the capture ELISA and TaqMan real-time RT-PCR. The log₁₀ values of the viral RNA copies/ml were calculated through interpolation of the Ct values from the standard curve. Serial dilutions of JS 52-3 with initial concentration of 10⁷ TCID₅₀ were captured by nMAb BB1A5. The dilution of 10² TCID₅₀ with a viral EV71 copy number of 59.84/ml still generated a detectable signal in the real-time PCR detection assay. These experiments were repeated three times and a representative result is shown. (C) Competitive ELISA test for anti-VP2 MAbs binding to EV71 virus. The dilution of nMAb BB1A5 (50 or 10 µg/well) and HBC-VP2(aa141-155) antisera competed with human serum samples for specifically binding to EV71 virus 52-3 coated on the well. The nonrelated monoclonal antibody and HBC(aa1-149) antisera were used as negative positive controls respectively. The anti-VP2 MAbs have been shown to block more than 60% of (EV71-infected) human sera from binding 52-3. (D) Reactivity of human serum (1:100 dilution) to VP2(aa141-155) epitope and EV71 strain JS 52-3. The clinical human serum samples used were well-characterized samples (Table 4).

TABLE 3. Oligonucleotide sequences of the primers used

Primer	Sequence
EV71-VP1-Forward	5'-CATATGGGAGATAGGGTGGCAGATG-3'
EV71-VP1-Reverse	5'-CTCGAGTTAAAGAGTAGTGATCGCTGTGC-3'
EV71-VP2-Forward	5'-CATATGTCCCCATCCGCTGAGG-3'
EV71-VP2-Reverse	5'-CTCGAGTTATTGCGTGACTGCCTGC-3'
EV71-VP3-Forward	5'-CATATGGGGTTTCCCACTGAGCTG-3'
EV71-VP3-Reverse	5'-CTCGAGTTACTGGATGGTGCCCGTCTG-3'
VP2(aa141-155)-Forward	5'-GATCCACGGAAGATAGTCACCCCTTACAAGCAGACTCAACCCGGCGCCG-3'
VP2(aa141-155)-Reverse	5'-AATTCGGCGCCGGTTGAGTCTGCTTGTAAGGGGGTGACTATCTCCGTG-3'

TABLE 4. The PCR detection and neutralization assay of human serum samples from patients with EV71

No. of sera	PCR detection		Neutralization titer	
	CA16	EV71	EV71	CA16
1	-	+	1024	0
2	-	+	1024	4096
3	-	+	256	0
4	-	+	512	0
5	-	+	256	32
6	-	+	2048	0
7	-	+	2048	0
8	-	+	2048	0

Discussion

Frequent HFMD epidemics caused by EV71 infection have created great public awareness and concerns over the past decade, especially in the Asia-Pacific region. Despite tremendous research efforts, there is still a lack of effective vaccines and treatment strategies against EV71 infections. The epitope peptide vaccine has represented a promising candidate for EV71 as the persistent research about effective immunogenic epitopes in recent years. Here we have derived with nMAb (BB1A5), mapped by

synthetic peptides and found to recognize an epitope spanning amino acids 141 to 155 within the VP2 capsid protein, enhanced in its immunogenicity by linkage to the MIR of hepatitis B virus core protein. Analysis of the serum of immunized mice showed EV71-neutralizing antibodies response to the VP2 epitope against wild-type EV71 strains from subgenogroups B3, B4, C2, C4 and C5. An oral EV71 mouse model was found to cause widely infection to many organs of mice, especially the CNS, then induce severe CNS symptoms and death[30]. Further researches have reported the possible pathway of EV71 infection to CNS through neural pathways[31]. Severe CNS involvement induced by EV71 infection have made the successful interruption of EV71 infection to CNS one of the major parts of vaccine protection. Through the *in vivo* passive protection assay, we found that the anti-HBc-VP2(aa141-155) antisera was not only able to protect the suckling mice from EV71-related CNS symptoms and death, but also successful in interrupting the spread of EV71 from the intestine to muscles and brains.

Despite high titers of specific antibodies generated by VP2-epitope, the potential for these MAbs to protect mice against lethal EV71 infection has been underappreciated. In part, this disregard is due to previous studies that failed to elicit virus neutralizing antibody response in mice[15, 23]. Recently, Ye *et al.*[32] showed that the possibility of using HBc-based VLPs for delivery of SP55 and SP70 epitopes of EV71 to achieve enhanced immunogenicity and protection against EV71 infection in the murine model. Moreover, they found that the divergent mechanism of neutralization and protection is in part attributed to their respective ability to bind authentic viral particles. Our data confirm that HBc-VP2(aa141-155)-immunized serum confer 100% *in vivo* passive protection when the newborn BALB/c mice are challenged with lethal pSVA-MP4. In contrast, anti-VP2(aa141-155) reacted with authentic viral particles (Fig. 9). Notably, *in vitro* studies of binding property of anti-VP2(aa141-155) have clearly shown that their attachment-blocking effect and provided certain foundations in the development of VP2(aa141-155) based epitope vaccine.

We have provided a detailed characterization of the cross-neutralizing epitope of VP2 between the mature virion and the expanded particle by using the high-resolution structures of EV71, which is helpful to understand the mechanisms of antibody-mediated neutralization and the dynamic process of EV71 entry. Wang *et al.*[11] have proposed a sensor-adaptor model in which receptor binding triggers virus uncoating. For EV71, it has been shown that human PSGL-1[33], scavenger receptor class B, member 2 (SCARB2)[34] and annexin II (Anx2)[35] are function-

al receptors for EV71 entry, and there may be more receptor molecules facilitate infection. The latest studies[36] have shown that EV71 binds to SCARB2 via a canyon or "pocket" region on the viral particle surface comprising residue Gln-172 and surrounding residues 163-177 of the capsid protein VP1 (green in Fig. 3C), and soluble SCARB2 could induce conformational changes of the viral capsid from 160 S to 135 S. Moreover, Anx2 as a cellular adherent factor that interacts with EV71 via the VP1 β -sheet (yellow in Fig. 3C) and the partial BC loop (residues 97-106) (orange in Fig. 3C)[35]. To develop a consistent naming of epitopes, the VP1 β -barrel, BC loop and surrounding residues 163-177 of VP1, which are part of the exposed outer capsid surrounding the 5-fold axis and form the "northern" rim of the canyon, will be defined as site 1. In the expanded particle, the EF loop of VP2, the GH loop of VP1 and VP3 lie in the area surrounding the second hole will be named site 2; and the pair of VP2 α A helices at the two-fold axis will be named site 3.

A previous study revealed that two peptides, SP55 and SP70, containing residues 163-177 of VP1 and the VP1 GH loop (residues 208-222) observed in site 1 and 2, respectively, are as efficient as the whole virion in eliciting neutralizing antibodies against EV71[14]. In our studies, the cross-neutralizing epitope of VP2 is located midway between site 1 and 3, adjacent to the VP1 GH loop (residues 208-222) and is able to confer effective *in vivo* passive protection against EV71 strains in suckling BALB/c mice. These states allow us to propose a multiple receptors mediated model in which SCARB2 or Anx2 may induce the conformational rearrangement of site 1, which in turns triggers the expulsion of the pocket factor, and serve as a primary receptor for the initial expansion of EV71 particles in preparation for further contact with a secondary receptor; upon expansion, the VP2 EF loop (site 2) might contribute to a bridge that drives the separation of the VP2 α A helices while the larger might also allow the exit of RNA (Fig. 10). Although, it is still unknown how the conformational changes trigger release of the viral genome into the cell.

It has been proposed that antibody-mediated neutralization of picornaviruses can inhibit infectivity via a number of different mechanisms[37]. Consideration of the results of this study suggests that the mechanism of EV71 neutralization *in vitro* might neutralize virions by stabilizing the capsid, which might then prevent uncoating or conformational changes in capsid morphology. Notably, neutralizing antibodies elicited by VP2 epitope may bind to the surface of EV71, and contact with the south wall of the canyon. In the process of expansion, VP2 epitope undergoes a separation, where C α movements reach ~ 4.4 Å. In addition, the expansion also results in a marked con-

formational change in the GH loop of VP3 and the appearance of a second hole[11]. It is possible that occupancy of the VP2 EF loop overlaps with the GH loop of VP1 and VP3 where lie in the area surrounding the second hole, and may prevents a necessary

conformational change in the site 2. Therefore, the stabilization of virions by antibodies is probably mediated by direct contact with the site 2 or "southern rim" of the canyon region, and then inhibits the expansion process of EV71 (Fig. 10).

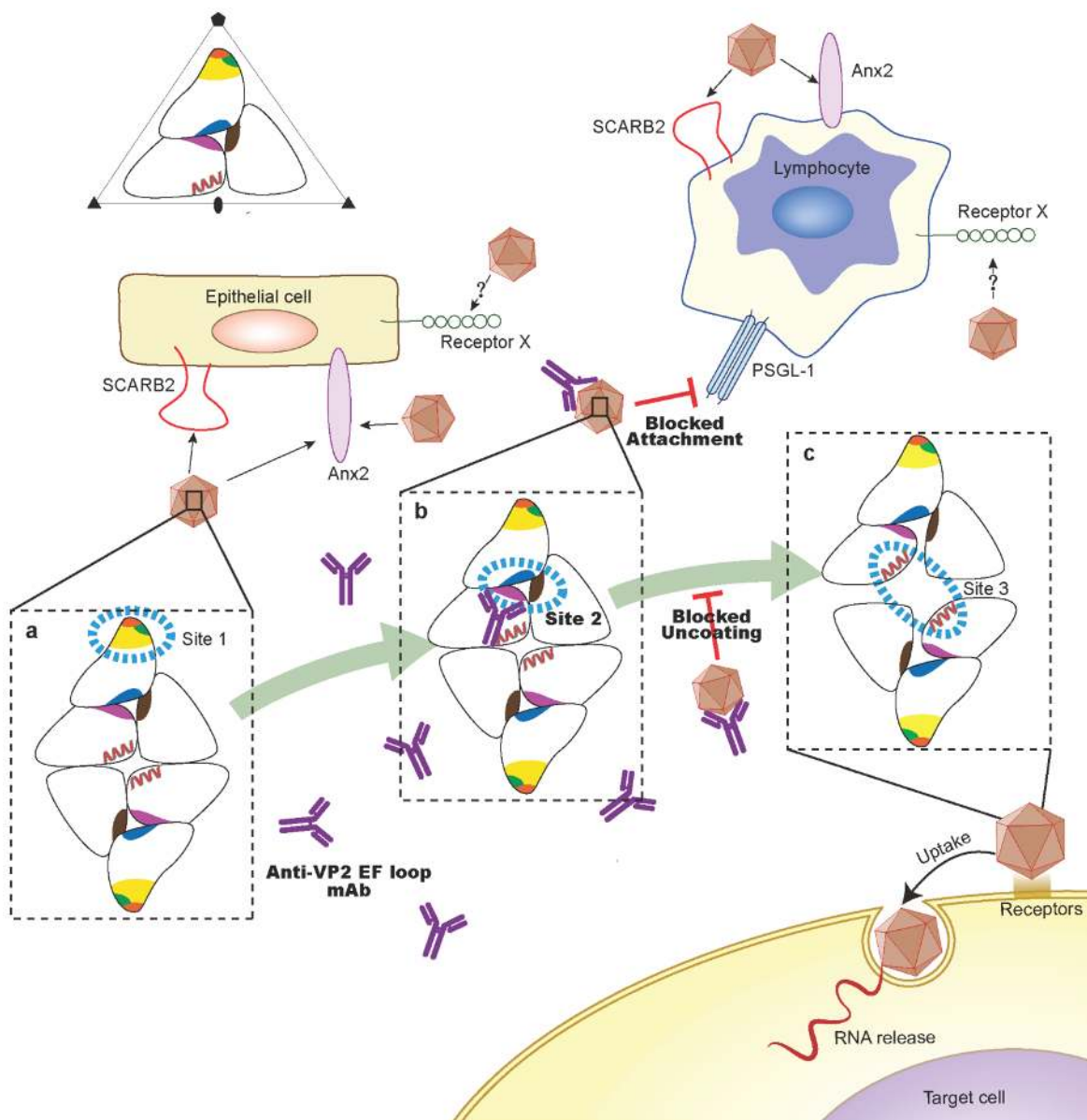


Fig. 10. A schematic representation showing the putative protective mechanism of VP2-epitope specific antibodies. According to the structure in Figure 7, a portion of the capsid is shown to depict the model of EV71 uncoating which we proposed (a-c). The positions of VP1, VP2, and VP3 that form a single protomer are indicated in relation to the twofold, threefold, and fivefold axes of symmetry of the particle. The positions of the defined site1-3 are indicated by blue dashed lines. The VP1 β -barrel, BC loop and surrounding residues 163-177 of VP1 from site 1 are indicated by yellow, orange, and green, respectively. The EF loop of VP2, the GH loop of VP1 and VP3, which lie in the area surrounding the second hole, are indicated in magenta, marine, firebrick, respectively. The pair of VP2 α A helices from site 3 is shown in red. We propose a multiple receptors mediated model: SCARB2 or Anx2 is widely expressed in epithelial cell lines, which may serve as a primary receptor for the initial expansion of EV71 particles and induce the conformational rearrangement of site 1; upon expansion, the VP2 EF loop (site 2) may contribute to a bridge. PSGL-1 may bind to the site 2 and interact with the SCARB2, Anx2 or another unidentified receptor, which act as the possible secondary receptor to facilitate the expansion process. The mechanisms for VP2 antibodies mediated EV71 neutralization *in vitro* might neutralize virions by stabilizing the capsid or block the PSGL-1-mediated viral infection process.

It has also been suggested that VP2 antibodies might neutralize infectivity by interfering with the attachment of EV71 virions to cellular. A large number of enteroviruses and rhinoviruses use a canyon-like feature on their surface to attach to cellu-

lar receptors. Binding into the canyon appears to be essential for the the uncoating process and the proper release of RNA into the cytoplasm of the host cell. Examples are human rhinoviruses and coxsackievirus A21 in complex with intracellular adhesion mole-

cule-1 (ICAM-1)[38, 39], poliovirus in complex with poliovirus receptor (PVR)[40, 41] and coxsackievirus B3 (CVB3) in complex with coxsackievirus-adenovirus receptor (CAR)[42]. Previous studies have demonstrated that the protruded E-F loop region of VP2, which is especially variable in VP2 of picornaviruses, is one of the large contact regions between PV and PVR and between CVA21 and its receptor ICAM-1[38]. In addition, the interface between the virus and the CAR receptor consists of the south rim of the canyon and belong to the puff region of VP2 between β E and α B[42, 43]. This region forms the part of neutralizing site 2 for the binding of neutralizing antibodies in PV[44]. We have shown that Lys149 side chains reposition plays a critical role in the conformational rearrangement of VP2 epitope. Because of Lys149 in the puff was a potential determinant for the human PSGL-1 interacts with EV71[45], the footprints of the PSGL-1 and VP2 antibody binding sites may overlap on the viral surface. In addition, PSGL-1 may bind to the VP2 EF loop (site 2) and interact with the SCARB2, Anx2 or another unidentified receptor, which act as the possible secondary receptor to facilitate the early stages of EV71 uncoating and infection. Therefore, VP2 antibodies are likely to block the PSGL-1-mediated viral infection process via steric hindrance (Fig. 10). Further cryo-electron microscopy (cryoEM) studies of interactions of EV71 with VP2 antibodies and PSGL-1 receptor may provide precise mechanism of neutralization by VP2 antibodies.

Hepatitis B virus core (HBc) protein was first reported as a promising VLP carrier in 1986 and was one of the most promising delivery vehicles of foreign epitopes suitable for designing highly immunogenic vaccines[46]. At present, the malaria vaccine candidate ICC-1132 and the flu vaccine candidate ACAM-FLU-ATM using HBc particles as an immune vehicle have completed phase I clinical trials[47, 48]. In general, HBc particles not only possess an outstanding ability to induce strong B cell, T cell and CTL responses, but also can act as a T-cell-independent and a T-cell-dependent antigen, which activates B cells directly[49]. In addition, N- or C-terminal regions, as well as the immunodominant loop in the MIR region of the HBc protein are accepted widely as targets for the introduction of foreign epitopes, ensuring retention and even enhancement of the avidity for the inserted epitope[50]. Results from our study demonstrated that the cross-neutralizing epitope of VP2 inserted into the MIR region of the HBc protein(aa1-149) does not interfere with particle formation, a prerequisite for the high immunogenicity of HBc fusion products, and can elicit good neutralizing antibody responses. In further study, we may need to evaluate various parameters to increase the immu-

nogenicity of the chimeric HBc-VP2(aa141-155) particles, such as different molecular constructs, adjuvants, and routes of administration. Specifically, an additional insertion of EV71-specific T cell or B cell epitopes into the fusion protein or put other neutralizing epitopes of EV71 into the chimeric HBc particles may improve the protective immunity. On the other hand, to insert repeats of the VP2 epitope may increase the immune response.

In the absence of a vaccine for EV71, our study has demonstrated that the *in vivo* passive protection of suckling BALB/c mice by antisera raised against the HBc-VP2(aa141-155) fusion protein offers a potential therapeutic treatment for EV71 infections. The Fab region of the mouse anti-VP2(aa141-155) antibody which recognizes and binds to the cross-neutralizing linear VP2 epitope can be selected as a potential candidate for humanized antibody production. Human monoclonal antibodies are a promising and rapidly growing category of targeted therapeutic agents, with 7 approved in the United States, 3 under review by the FDA, 7 in late-stage development and 81 in early-stage development[51]. The attributes of broad-spectrum neutralizing activity, target specificity and the ability to activate the immune system suggest that the continuing promise of therapeutic antibodies against EV71 infection.

Abbreviations

EV71: enterovirus 71; HFMD: hand, foot, and mouth disease; HBc: hepatitis B virus core protein; PV1: poliovirus type 1; CAV9: coxsackie A9; nMAb: neutralizing monoclonal antibody; ATCC: American Type Culture Collection; CPE: cytopathic effects; TCID50: 50% tissue culture infectious doses; PB: phosphate buffer; HRP: horseradish peroxidase; IPTG: isopropylthio- β -D-galactopyranoside; HPLC: high performance liquid chromatogram; AKP: alkaline phosphatase; BCIP/NBT: bromochloroindole phosphate/nitro blue tetrazolium substrate; GAM-HRP: Horseradish peroxidase-conjugated goat anti-mouse; MIR: immunodominant region; IFA: immunofluorescence Assay; HE: hematoxylin and eosin; IHC: immunohistochemistry; ADCC: antibody-dependent cellular cytotoxicity; SCARB2: scavenger receptor class B, member 2; Anx2: annexin II; ICAM-1: intracellular adhesion molecule-1; PVR: poliovirus receptor; CVB3: coxsackievirus B3; CAR: coxsackievirus-adenovirus receptor; Cryo-EM: cryo-electron microscopy.

Acknowledgments

This work was supported by a grant from the National Science and Technology Major Project of the Ministry of Science and Technology of China (No.

2010ZX09401-403), National Natural Science Foundation of China (No. 30972826) and National Natural Science Fund for Distinguished Young Scholar (No.30925030). The funders had no role in study design, data collection and analysis, decision to publish, or preparation of the manuscript.

Competing Interests

The authors have declared that no competing interest exists.

References

- Patel KP, Bergelson JM. Receptors identified for hand, foot and mouth virus. *Nat Med.* 2009; 15: 728-9.
- Hagiwara A, Tagaya I, Yoneyama T. Epidemic of hand, foot and mouth disease associated with enterovirus 71 infection. *Intervirology.* 1978; 9: 60-3.
- Ishimaru Y, Nakano S, Yamaoka K, Takami S. Outbreaks of hand, foot, and mouth disease by enterovirus 71. High incidence of complication disorders of central nervous system. *Arch Dis Child.* 1980; 55: 583-8.
- Ooi MH, Wong SC, Lewthwaite P, Cardoso MJ, Solomon T. Clinical features, diagnosis, and management of enterovirus 71. *Lancet Neurol.* 2010; 9: 1097-105.
- Xu J, Qian Y, Wang S, Serrano JM, Li W, Huang Z, et al. EV71: an emerging infectious disease vaccine target in the Far East? *Vaccine.* 2010; 28: 3516-21.
- Chumakov M, Voroshilova M, Shindarov L, Lavrova I, Gracheva L, Koroleva G, et al. Enterovirus 71 isolated from cases of epidemic poliomyelitis-like disease in Bulgaria. *Arch Virol.* 1979; 60: 329-40.
- Nagy G, Takatsy S, Kukan E, Mihaly I, Domok I. Virological diagnosis of enterovirus type 71 infections: experiences gained during an epidemic of acute CNS diseases in Hungary in 1978. *Arch Virol.* 1982; 71: 217-27.
- Chan LG, Parashar UD, Lye MS, Ong FG, Zaki SR, Alexander JP, et al. Deaths of children during an outbreak of hand, foot, and mouth disease in sarawak, malaysia: clinical and pathological characteristics of the disease. For the Outbreak Study Group. *Clin Infect Dis.* 2000; 31: 678-83.
- Chang LY. Enterovirus 71 in Taiwan. *Pediatr Neonatol.* 2008; 49: 103-12.
- Cardoso MJ, Perera D, Brown BA, Cheon D, Chan HM, Chan KP, et al. Molecular epidemiology of human enterovirus 71 strains and recent outbreaks in the Asia-Pacific region: comparative analysis of the VP1 and VP4 genes. *Emerg Infect Dis.* 2003; 9: 461-8.
- Wang X, Peng W, Ren J, Hu Z, Xu J, Lou Z, et al. A sensor-adaptor mechanism for enterovirus uncoating from structures of EV71. *Nat Struct Mol Biol.* 2012; 19: 424-9.
- Plevka P, Perera R, Cardoso J, Kuhn RJ, Rossmann MG. Crystal Structure of Human Enterovirus 71. *Science.* 2012; doi:10.1126/science.1218713.
- Rossmann MG, Arnold E, Erickson JW, Frankenberger EA, Griffith JP, Hecht HJ, et al. Structure of a human common cold virus and functional relationship to other picornaviruses. *Nature.* 1985; 317: 145-53.
- Foo DG, Alonso S, Phoon MC, Ramachandran NP, Chow VT, Poh CL. Identification of neutralizing linear epitopes from the VP1 capsid protein of Enterovirus 71 using synthetic peptides. *Virus Res.* 2007; 125: 61-8.
- Liu CC, Chou AH, Lien SP, Lin HY, Liu SJ, Chang JY, et al. Identification and characterization of a cross-neutralization epitope of Enterovirus 71. *Vaccine.* 2011; 29: 4362-72.
- Fiore L, Ridolfi B, Genovese D, Buttinelli G, Lucioi S, Lahm A, et al. Poliovirus Sabin type 1 neutralization epitopes recognized by immunoglobulin A monoclonal antibodies. *J Virol.* 1997; 71: 6905-12.
- Buttinelli G, Donati V, Ruggeri FM, Joki-Korpela P, Hyypia T, Fiore L. Antigenic sites of coxsackie A9 virus inducing neutralizing monoclonal antibodies protective in mice. *Virology.* 2003; 312: 74-83.
- Bubeck D, Filman DJ, Cheng N, Steven AC, Hogle JM, Belnap DM. The structure of the poliovirus 135S cell entry intermediate at 10-angstrom resolution reveals the location of an externalized polypeptide that binds to membranes. *J Virol.* 2005; 79: 7745-55.
- Lin J, Cheng N, Chow M, Filman DJ, Steven AC, Hogle JM, et al. An externalized polypeptide partitions between two distinct sites on genome-released poliovirus particles. *J Virol.* 2011; 85: 9974-83.
- Zhang D, Lu J. Enterovirus 71 vaccine: close but still far. *Int J Infect Dis.* 2010; 14: e739-43.
- Foo DG, Macary PA, Alonso S, Poh CL. Identification of human CD4 T-cell epitopes on the VP1 capsid protein of enterovirus 71. *Viral Immunol.* 2008; 21: 215-24.
- Foo DG, Alonso S, Chow VT, Poh CL. Passive protection against lethal enterovirus 71 infection in newborn mice by neutralizing antibodies elicited by a synthetic peptide. *Microbes Infect.* 2007; 9: 1299-306.
- Kiener TK, Jia Q, Lim XF, He F, Meng T, Chow VT, et al. Characterization and specificity of the linear epitope of the enterovirus 71 VP2 protein. *Virol J.* 2012; 9: 55.
- Kohler G, Milstein C. Continuous cultures of fused cells secreting antibody of predefined specificity. *Nature.* 1975; 256: 495-7.
- Galfre G, Howe SC, Milstein C, Butcher GW, Howard JC. Antibodies to major histocompatibility antigens produced by hybrid cell lines. *Nature.* 1977; 266: 550-2.
- Luo WX, Zhang J, Yang HJ, Li SW, Xie XY, Pang SQ, et al. [Construction and application of an Escherichia coli high effective expression vector with an enhancer]. *Sheng Wu Gong Cheng Xue Bao.* 2000; 16: 578-81.
- Yang HJ, Chen M, Cheng T, He SZ, Li SW, Guan BQ, et al. Expression and immunoactivity of chimeric particulate antigens of receptor binding site-core antigen of hepatitis B virus. *World J Gastroenterol.* 2005; 11: 492-7.
- Xu F, Yan Q, Wang H, Niu J, Li L, Zhu F, et al. Performance of detecting IgM antibodies against enterovirus 71 for early diagnosis. *PLoS One.* 2010; 5: e11388.
- Xu F, He D, He S, Wu B, Guan L, Niu J, et al. Development of an IgM-capture ELISA for Coxsackievirus A16 infection. *J Virol Methods.* 2011; 171: 107-10.
- Wang YF, Chou CT, Lei HY, Liu CC, Wang SM, Yan JJ, et al. A mouse-adapted enterovirus 71 strain causes neurological disease in mice after oral infection. *J Virol.* 2004; 78: 7916-24.
- Chen CS, Yao YC, Lin SC, Lee YP, Wang YF, Wang JR, et al. Retrograde axonal transport: a major transmission route of enterovirus 71 in mice. *J Virol.* 2007; 81: 8996-9003.
- Ye X, Ku Z, Liu Q, Wang X, Shi J, Zhang Y, et al. Chimeric Virus-Like Particle Vaccines Displaying Conserved Enterovirus 71 Epitopes Elicit Protective Neutralizing Antibodies in Mice through Divergent Mechanisms. *J Virol.* 2014; 88: 72-81.
- Nishimura Y, Shimojima M, Tano Y, Miyamura T, Wakita T, Shimizu H. Human P-selectin glycoprotein ligand-1 is a functional receptor for enterovirus 71. *Nat Med.* 2009; 15: 794-7.
- Yamayoshi S, Yamashita Y, Li J, Hanagata N, Minowa T, Takemura T, et al. Scavenger receptor B2 is a cellular receptor for enterovirus 71. *Nat Med.* 2009; 15: 798-801.
- Yang SL, Chou YT, Wu CN, Ho MS. Annexin II binds to capsid protein VP1 of enterovirus 71 and enhances viral infectivity. *J Virol.* 2011; 85: 11809-20.
- Chen P, Song Z, Qi Y, Feng X, Xu N, Sun Y, et al. Molecular determinants of enterovirus 71 viral entry: cleft around GLN-172 on VP1 protein interacts with variable region on scavenger receptor B 2. *J Biol Chem.* 2012; 287: 6406-20.
- Che Z, Olson NH, Leippe D, Lee WM, Mosser AG, Rueckert RR, et al. Antibody-mediated neutralization of human rhinovirus 14 explored by means of cryoelectron microscopy and X-ray crystallography of virus-Fab complexes. *J Virol.* 1998; 72: 4610-22.
- Xiao C, Bator CM, Bowman VD, Rieder E, He Y, Hebert B, et al. Interaction of coxsackievirus A21 with its cellular receptor, ICAM-1. *J Virol.* 2001; 75: 2444-51.
- Xiao C, Bator-Kelly CM, Rieder E, Chipman PR, Craig A, Kuhn RJ, et al. The crystal structure of coxsackievirus A21 and its interaction with ICAM-1. *Structure.* 2005; 13: 1019-33.
- Belnap DM, McDermott BM, Jr., Filman DJ, Cheng N, Trus BL, Zuccola HJ, et al. Three-dimensional structure of poliovirus receptor bound to poliovirus. *Proc Natl Acad Sci U S A.* 2000; 97: 73-8.
- He Y, Bowman VD, Mueller S, Bator CM, Bella J, Peng X, et al. Interaction of the poliovirus receptor with poliovirus. *Proc Natl Acad Sci U S A.* 2000; 97: 79-84.
- He Y, Chipman PR, Howitt J, Bator CM, Whitt MA, Baker TS, et al. Interaction of coxsackievirus B3 with the full length coxsackievirus-adenovirus receptor. *Nat Struct Biol.* 2001; 8: 874-8.
- Rossmann MG, He Y, Kuhn RJ. Picornavirus-receptor interactions. *Trends Microbiol.* 2002; 10: 324-31.
- Page GS, Mosser AG, Hogle JM, Filman DJ, Rueckert RR, Chow M. Three-dimensional structure of poliovirus serotype 1 neutralizing determinants. *J Virol.* 1988; 62: 1781-94.
- Miyamura K, Nishimura Y, Abo M, Wakita T, Shimizu H. Adaptive mutations in the genomes of enterovirus 71 strains following infection of mouse cells expressing human P-selectin glycoprotein ligand-1. *J Gen Virol.* 2011; 92: 287-91.
- Clarke BE, Newton SE, Carroll AR, Francis MJ, Appleyard G, Syred AD, et al. Improved immunogenicity of a peptide epitope after fusion to hepatitis B core protein. *Nature.* 1987; 330: 381-4.
- Schotsaert M, De Filette M, Fiers W, Saelens X. Universal M2 ectodomain-based influenza A vaccines: preclinical and clinical developments. *Expert Rev Vaccines.* 2009; 8: 499-508.
- Walther M, Dunachie S, Keating S, Vuola JM, Berthoud T, Schmidt A, et al. Safety, immunogenicity and efficacy of a pre-erythrocytic malaria candidate vaccine, ICC-1132 formulated in Seppic ISA 720. *Vaccine.* 2005; 23: 857-64.
- Milich DR, McLachlan A. The nucleocapsid of hepatitis B virus is both a T-cell-independent and a T-cell-dependent antigen. *Science.* 1986; 234: 1398-401.
- Pumpens P, Borisova GP, Crowther RA, Grens E. Hepatitis B virus core particles as epitope carriers. *Intervirology.* 1995; 38: 63-74.
- Nelson AL, Dhimoolea E, Reichert JM. Development trends for human monoclonal antibody therapeutics. *Nat Rev Drug Discov.* 2010; 9: 767-74.